Global Bioenergy Capacity as Constrained by Observed Biospheric Productivity Rates

W. KOLBY SMITH, MAOSHENG ZHAO, AND STEVEN W. RUNNING

Virtually all global energy forecasts include an expectation that bioenergy will be a substantial future energy source. However, the scale of this potential resource remains poorly understood because of uncertain land availability and yield expectations. Here, we used climate-constrained, satellite-derived net primary productivity data computed for 110 million square kilometers of terrestrial plant production as an upper-envelope constraint on primary bioenergy potential (PBP). We estimated the maximum PBP to realistically range from 12% to 35% of 2009 global primary energy consumption, with yield potential ranging from 6.6 to 18.8 megajoules per square meter per year—roughly four times lower than previous evaluations. Our results highlight many recent bioenergy evaluations as overoptimistic, which we attribute to a failure to adequately apply biophysical constraints in estimates of yield potential. We do not advocate bioenergy production at the levels reported in this analysis; instead, we simply report the ceiling for PBP based on current planetary productivity.

Keywords: carbon, bioenergy, energy, global, land use

Climate change policy and concerns regarding future energy security continue to stimulate an unprecedented rise in the production of bioenergy—a renewable energy source with the potential to reduce greenhouse gas emissions (Haberl et al. 2010, Chum et al. 2011). However, determining the scale at which bioenergy can be sustained globally requires knowledge of two complex factors: (1) future land availability for bioenergy production and (2) future yield expectations (Haberl et al. 2010). These factors are not independent; yield potential greatly varies depending on land quality, which, in turn, is largely determined by biophysical (e.g., solar radiation, temperature, precipitation) as well as management (e.g., irrigation, fertilization) factors.

Numerous researchers have attempted to resolve bioenergy potential at the global scale using a wide range of methodologies. Most commonly, crop-specific average yield values recorded at the plot level have been applied across land areas considered suitable for bioenergy production (Hoogwijk et al. 2005, Smeets et al. 2007, van Vuuren et al. 2009, Pacca and Moreira 2011). However, this type of approach can greatly overestimate biofuel potential, because average yield values do not reflect variations driven by biophysical factors and management practices (Johnston et al. 2009). Others have applied process models that combine plot-level yield-potential estimates, spatially explicit climatic data, and management practices to more realistically estimate spatial variability in yield (Erb et al. 2009, Beringer et al. 2011). However, the results of these analyses are highly sensitive to crop type, extrapolation technique, and calibration data (Campbell et al. 2008, Field et al. 2008). Moreover, the ability to validate the performance of such a model is limited, because crop-specific field data remain sparsely available at the global scale (Campbell et al. 2008, Field et al. 2008). Currently, average yield-potential estimates reported in the literature vary by nearly an order of magnitude, from 6.9 to 60 megajoules (MJ) per square meter (m^2) per year (Haberl et al. 2010), which significantly contributes to variability in global bioenergy potential estimates, which have been documented to range from roughly 5% to as high as 300% of the 2009 global primary energy consumption (GPEC09; Haberl et al. 2010, USEIA 2011).

Reducing the range of variability associated with current estimates of bioenergy potential represents a significant first step toward a more quantitative understanding of the scale of bioenergy as a future energy source. Here, we estimate *primary bioenergy potential* (PBP)—or bioenergy potential before energy conversion losses (e.g., during liquefaction)—from satellite-derived net primary productivity (NPP) data (from NASA's Moderate-Resolution Imaging Spectroradiometer [MODIS]; see, e.g., Running et al. 2004, Zhao et al. 2005, Zhao and Running 2010). NPP varies as a function of multiple factors, including vegetation type, soil type, climate, and management (Vitousek et al. 1986, DeFries 2002, Haberl et al. 2007). At the global scale,

BioScience 62: 911–922. ISSN 0006-3568, electronic ISSN 1525-3244. doi:10.1525/bio.2012.62.10.11

however, the conversion of natural ecosystems to agricultural lands has been shown to result in significant reductions in NPP (Vitousek et al. 1986, DeFries 2002, Haberl et al. 2007). In fact, Haberl and colleagues (2007) estimated that large-scale cropland productivity is consistently lower than that of the natural vegetation it replaced, independent of landcover type or region. Only under intensive management (i.e., irrigation or fertilization), which is often limited to relatively small scales because of resource availability, has cropland productivity been shown to exceed that of the natural potential (DeFries 2002, Haberl et al. 2007). However, even in these relatively localized cases, DeFries (2002) showed that cropland productivity does not exceed decadal-scale variability in natural productivity, which reveals the limited potential for increasing productivity beyond that of the natural vegetation. Because current bioenergy systems are subject to similar agriculture-based management practices, we argue that constraining yield potential to natural observed rates of NPP represents a realistic upper-envelope evaluation of PBP.

Our use of MODIS-derived NPP quantifies current terrestrial biomass growth capacity for every square kilometer (km^2) of the entire 110 million km^2 of vegetated Earth by integrating remotely sensed vegetation dynamics (e.g., the fraction of photosynthetically active radiation and leaf area index data) and global climatic data (e.g., temperature and moisture; Zhao et al. 2005). Using MODIS-derived NPP in a top-down evaluation of PBP removes the need for extrapolation of plot-level observed yields, which, as was mentioned above, generally overestimates PBP. Satellite data has been previously used to assess the bioenergy potential of abandoned agricultural land, as was described by Campbell and colleagues (2008) and by Field and colleagues (2008). Our analysis builds on these previous studies in that we consider all vegetation and then systematically remove landcover types according to current availability. Thus, we provide a continuous quantification of PBP across broad land-use scenarios, which elucidates the relationship between land availability and yield potential and allows for comparison across all current bioenergy analyses, independent of land-use assumptions. Ultimately, our objective with this study is to estimate the upper envelope for global bioenergy production across future land-use options, using MODIS NPP as the most geographically explicit measure of the current growth capacity of the terrestrial biosphere (Running et al. 2004, Zhao et al. 2005, Zhao and Running 2010).

Calculating global bioenergy capacity from satellite data

In the following sections, we describe the approach we followed in calculating global bioenergy capacity.

Global satellite-derived vegetation productivity. We started our analysis with MODIS NPP data as a fundamental constraint on global bioenergy potential (Running et al. 2004, Zhao et al. 2005, Zhao and Running 2010, Smith et al. 2012). The MODIS NPP algorithm, as was described by Running and colleagues (2004), was used to calculate the 2000–2010 MODIS NPP with a 1-km^2 resolution. Eight-day composite 1-km^2-resolution fraction of photosynthetically active radiation and leaf area index MODIS Collection 5 data products were used as remotely sensed vegetation property dynamic inputs (Running et al. 2004). For the daily meteorological variables required to drive the algorithm, we used data obtained from the Data Assimilation Office data sets (Schubert et al. 1993). The 2000–2010 MODIS NPP data were averaged and aggregated to a 10-km^2 spatial resolution (figure 1). For more detail, as well as a validation of the MODIS GPP/NPP algorithm, see Running and colleagues (2004), Zhao and colleagues (2005), and Zhao and Running (2010, 2011).

Global landcover classification. We used a 10-km^2-resolution composite landcover classification consisting of socioeconomically relevant land-use types, including cropland, pastureland, forestland, rangeland, protected land, and low-productivity land (figure 1). We did not consider urban-dominated or barren landcover classes, because they contribute negligibly to global vegetation productivity (Zhao et al. 2005); our definition is based on University of Maryland (UM) MODIS landcover data (Friedl et al. 2010). Data from Ramankutty and colleagues (2008) were used as the basis for our crop- and pastureland definition. Ramankutty and colleagues (2008) defined *cropland* to include permanent and temporarily (less than 5 years) fallow croplands only, whereas *pastureland* was defined to include permanent (more than 5 years) pasturelands specifically managed for livestock grazing. For both crop- and pasturelands, we converted percentage-coverage data to discrete data using a 40% occupancy threshold, meaning that a given pixel was reclassified as *occupied* if the landcover type of interest had a percentage coverage greater than or equal to the threshold. In the case in which both crop and pasture coverage was greater than or equal to the threshold, the pixel was characterized according to the landcover type with the greater percentage coverage. *Forestland* was defined with UM MODIS landcover data (Friedl et al. 2010) as the combination of evergreen needleleaf, evergreen broadleaf, deciduous needleleaf, deciduous broadleaf, and mixed forest landcover types. *Rangeland* was classified as all remaining vegetated (i.e., not barren) land as defined by UM MODIS landcover data (Friedl et al. 2010).

In addition, we partitioned natural landcover types (i.e., forests and rangelands) as either *accessible* or *remote* (figure 1), using human footprint index data set, which accounts for accessibility by incorporating information on roads, major rivers, and coastlines (SEDAC 2005). *Remote* lands represent the lowest 15% of human index scores, which is roughly equivalent to the 15% least accessible land globally (SEDAC 2005). *Protected* regions were classified as only areas of strict protection, including national parks and nature reserves, according to World Database on Protected Areas data (*www.*

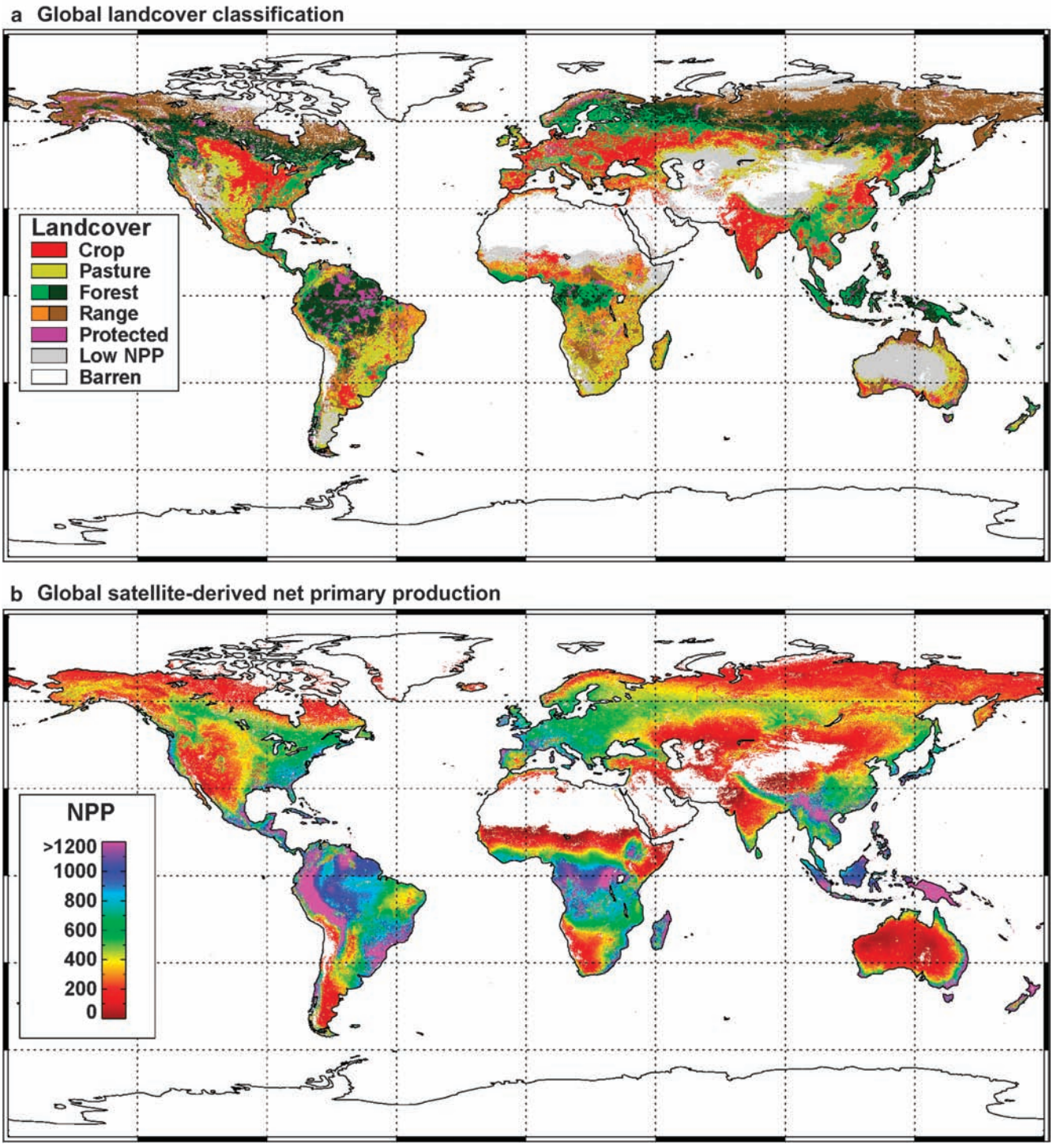

Figure 1. Global landcover and net primary productivity (NPP). (a) Global landcover divided into crop, pasture, forest, range, protected, low-NPP (i.e., low-productivity land), and barren landcover classes. The forests and rangelands are partitioned into* accessible *and* remote *land, designated by light and dark shades, respectively. (b) Global NPP (in grams of carbon per square meter per year) averaged from 2000 to 2010, estimated from the MODIS (Moderate-Resolution Imaging Spectroradiometer) NPP algorithm (see the text) at a 10-square-kilometer spatial resolution (Running et al. 2004, Zhao et al. 2005, Zhao and Running 2010, 2011).

wdpa.org). Finally, we classified *low-productivity* land using a productivity threshold of 150 grams (g) of carbon per m^2 per year, the threshold at which harvest energy inputs (e.g., establishment, management, harvest) exceed potential energy outputs (Nonhebel 2002, Schmer et al. 2008). The resulting area, considered *low productivity*, was estimated to

extend 20.3 million km^2 (figure 1), which is consistent with the estimates of roughly 16 million km^2 and 24 million km^2 reported by Haberl and colleagues (2011) and Chum and colleagues (2011), respectively.

Current agricultural and forestry harvest. Current agricultural and forestry harvest was assumed to occur only on croplands and accessible forestlands. We estimated agricultural and forestry harvest rates as a proportion of MODIS NPP according to current harvest statistics (*http://faostat.fao.org*). Four relevant harvest pools were considered: (1) *total harvest* (H_{TOTAL}), or total aboveground biomass at the time of harvest; (2) *recoverable harvest* (H_{REC}), or the fraction of H_{TOTAL} removed from the field at the time of harvest; (3) *harvest losses* (H_{LOSS}), or the fraction of H_{TOTAL} remaining in the field postharvest; and (4) *harvest residues* (H_{RES}), or the fraction of H_{LOSS} recoverable without affecting nutrient cycling (primary residues; e.g., felled branches) plus the fraction of H_{REC} unused following harvest processing (secondary residues; e.g., sawdust). Harvest pools were estimated at a spatial resolution of 10 km^2 in the manner described in box 1.

Maximum sustainable agricultural and forestry harvest. The *maximum sustainable harvest* (MSH)—defined as the maximum possible harvest without affecting future yields and nutrient cycling—was estimated for potential agricultural land (i.e., current cropland, pastureland, accessible range, and remote range) and potential forestry land (i.e., accessible forests and remote forests) according to box 1. We did not consider the conversion of forest to agricultural land, because it has been well documented that this type of landcover conversion results in a net detrimental climate change impact (Tilman et al. 2009). MSH pools (MSH_{TOTAL}, MSH_{REC}, MSH_{LOSS}, MSH_{RES}) were calculated by simply replacing the current total harvest ratio (y_{rec}; see box 1) with a literature-derived *MSH* ratio (y_{msh}). For agricultural systems, a maximum y_{msh} of 1.00 (with a range of .90–1.00) was used, because all aboveground biomass on croplands is generally either harvested or decomposed annually (see supplemental table S1, available online at *http://dx.doi.org/10.1525/bio.2012.62.8.11*). For forest systems, a y_{msh} of .20 (with a range of .15–.25) was used on the basis of current global forestry harvest trends (table S1). We used an MSH value for forestry systems that is consistent with the highest current global forestry harvest rates, which resulted in a more than twofold increase in global forest harvest (table S3).

Primary bioenergy potential. We estimated PBP as a function of landcover class using four land-use scenarios (table 1): (1) As a starting point, we estimated the biospheric capacity for bioenergy over all vegetated land (PBP_{CAP}; figure 2a). (2) From PBP_{CAP}, we calculated bioenergy potential with maximum use of available land (PBP_{MAX}; figure 2b) by removing all *unavailable* sources, defined to include current crop and forestry harvest, protected areas, and low-productivity land. (3) From PBP_{MAX}, we next estimated bioenergy potential with only moderate land use (PBP_{MOD}; figure 2c) by removing *low-availability* sources, defined to include pastures, remote regions, and accessible forestland. (4) Finally, we calculated bioenergy potential with minimum land use by considering only *immediately available* sources (PBP_{MIN}; figure 2d), defined to

Box 1. Calculating current agricultural and forestry harvest.

Harvest (H) pools, including total harvest (H_{TOTAL}), recoverable harvest (H_{REC}), harvest losses (H_{LOSS}), and harvest residues (H_{RES}), were estimated at a spatial resolution of 10 square kilometers according to the equations below. For the total harvest,

$$H_{TOTAL} = \sum(\text{NPP} \times \text{r}_{abv} \times \text{y}_{total}), \quad (1)$$

where r_{abv} and y_{total} represent literature-derived aboveground net primary productivity and total aboveground yield-potential ratios, respectively. For agricultural harvest, r_{abv} and y_{total} were estimated as .83 (with a range of .80–.85) and 1.00 (with a range of .90–1.00), respectively, which represents the global average for four dominant global crops (i.e., maize, rice, wheat, and soybean), accounting for 70% of global agricultural land (Roy et al. 2001, Monfreda et al. 2008). Because of significant spatial variability in forestry harvest, r_{abv} and y_{total} were estimated regionally (figure S1; UNSD 2011) according to literature-derived aboveground ratios and average harvest volume data (see supplemental table S1, available online at *http://dx.doi.org/10.1525/bio.2012.62.8.11*; Roy et al. 2001, *http://faostat.fao.org*). H_{TOTAL} was calculated as the sum of all agricultural or forestry pixels (n). H_{REC}, H_{LOSS}, and H_{RES} were estimated as proportional to H_{TOTAL}, according to equations 2–4:

$$H_{REC} = \sum[H_{TOTAL} \times y_{rec} \times (1 - y_{res2})], \quad (2)$$

$$H_{LOSS} = \sum[H_{TOTAL} \times (1 - y_{rec}) \times (1 - y_{res1})], \quad (3)$$

$$H_{RES} = \sum[H_{TOTAL} \times (1 - y_{rec}) \times y_{res1} + H_{TOTAL} \times y_{rec} \times y_{res2}], \quad (4)$$

where y_{rec}, y_{res1}, and y_{res2} represent literature-derived yield-potential ratios describing the average proportion of H_{TOTAL} recovered at the time of harvest, the proportion of H_{LOSS} recoverable without affecting nutrient cycling (primary residuals), and the proportion of H_{REC} available following harvest processing (secondary residuals), respectively. For agricultural harvest, y_{rec} and y_{res2} were estimated to be .50 (range = .40–.60) and .10 (range = .05–.15), respectively (Monfreda et al. 2008). For forest harvest, y_{rec} and y_{res2} were estimated to be .80 (range = .70–.90) and .40 (range = .30–.50), respectively (Haberl et al. 2007, Smeets et al. 2007). Finally, y_{res1} was estimated to be .30 (range = .25–.35) for both agricultural and forestry harvest (Smeets et al. 2007, Gregg and Smith 2010). A summary of the calculated global agricultural and forestry harvest pools is presented as a function of region in tables S2 and S3, respectively. Also, a spatial representation of total harvest (H_{TOTAL}) is shown in figure S2. For additional methodological details, see Smith and colleagues (2012).

include only current crop and forest harvest residuals. The PBP pools were estimated at a spatial resolution of 10 km^2 in the manner described in box 2.

Energy conversion. We then applied well-known energy conversion constants according to equation 7 below (see boxes 1 and 2 for equations 1–6) in order to estimate *energy* (in joules [J] per year) from *biomass* (in grams of carbon per year) assuming a 0.45 carbon-to-biomass ratio ($CR_{biomass}$; Williams et al. 1987) and an 18-MJ-per-kilogram gross biomass energy content (CF_{energy}; Tsubo et al. 2001). We considered only primary energy and, therefore, did not take into account energy losses due to energy conversion.

$$energy = (biomass \times CF_{energy}) / CR_{biomass}, \quad (7)$$

Table 1. Land-use scenarios used to evaluate primary bioenergy potential.

Land-use scenario	Definition	Sources considered
Biospheric capacity (PBP_{CAP})	All vegetated land	—
Maximum land use (PBP_{MAX})	PBP_{CAP} without unavailable sources[a]	Pastures, remote regions, accessible forests, accessible rangelands, crop and forestry harvest residues
Moderate land use (PBP_{MOD})	PBP_{MAX} without low-availability sources[b]	Accessible rangelands, crop and forestry harvest residues
Minimum land use (PBP_{MIN})	Immediately available sources[c] only	Crop and forestry harvest residues

[a] *Unavailable sources* were defined to include current crop and forest harvest, protected land, and low-productivity land.
[b] *Low availability sources* were defined to include current pastures, remote regions, and accessible forests.
[c] *Immediately available sources* were defined to include crop and forest harvest residues only.

Current global harvest

We estimated global NPP, averaged from 2000 to 2010, to be 53.1 petagrams (Pg) of carbon (C) per year over 110.1 million km^2 (table 2, figure 1), which is

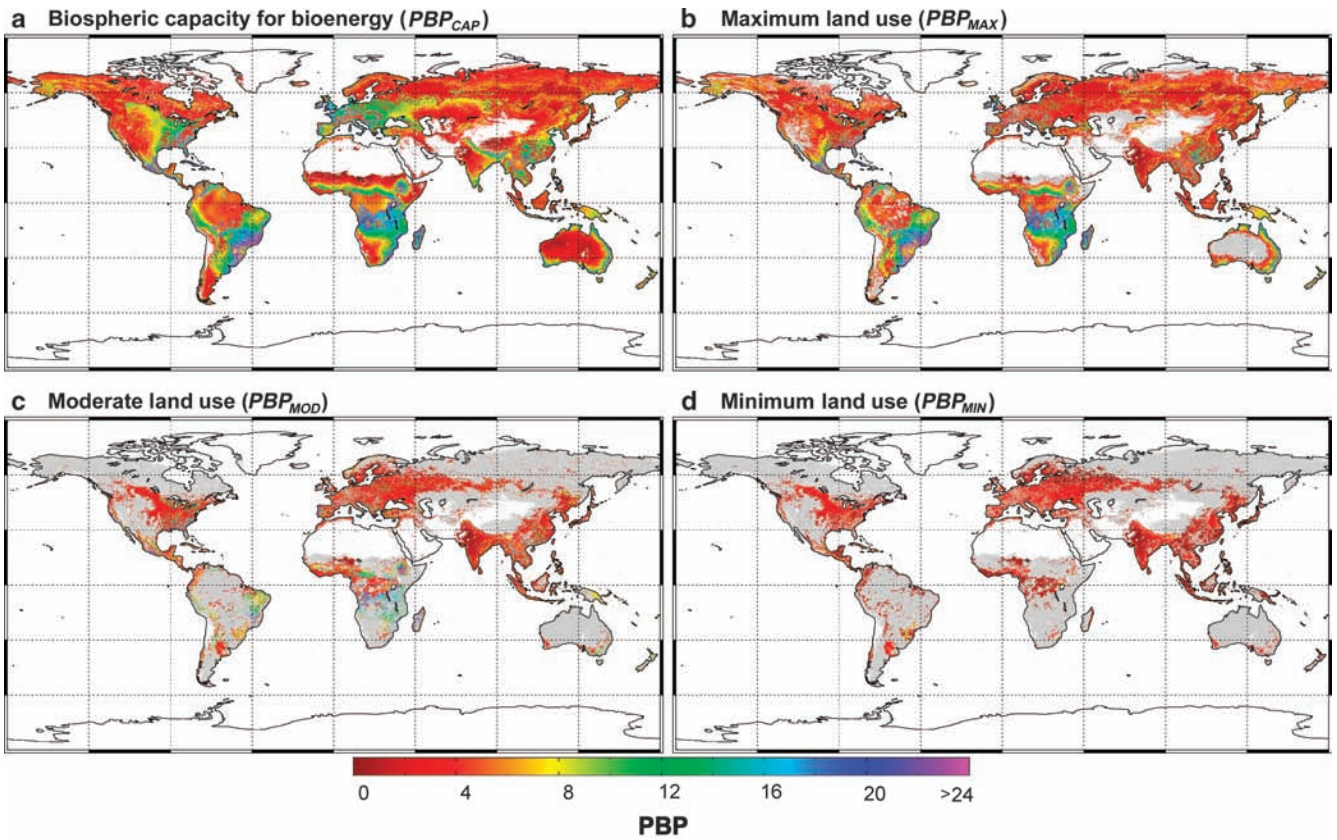

Figure 2. Spatially explicit primary bioenergy potential (PBP; in megajoules per square meter per year) as a function of land-use scenario. (a) Biospheric capacity for bioenergy (PBP_{CAP}). PBP_{CAP} represents the conversion of all terrestrial primary production to bioenergy (table 1). (b) Maximum land use (PBP_{MAX}). We defined PBP_{MAX} to exclude unavailable sources, including current crop and forest harvest, protected regions, and land under a minimum productivity threshold (table 1). (c) Moderate land use (PBP_{MOD}). We defined PBP_{MOD} to exclude unavailable sources and low-availability sources, including remote regions and pasturelands (table 1). (d) Minimum land use (PBP_{MIN}). PBP_{MIN} represents a land-use scenario in which only immediately available sources, including current harvest residuals, are used for bioenergy production (table 1). PBP_{MIN} has the benefit of requiring no additional harvest land.

Box 2. Calculating primary bioenergy potential.

Primary bioenergy potential (*PBP*) scenarios, including the biospheric capacity (PBP_{CAP}), maximum land use (PBP_{MAX}), moderate land use (PBP_{MOD}), and minimum land use (PBP_{MIN}), were estimated at a spatial resolution of 10 square kilometers according to equations 5–6:

$$PBP_{CAP}/PBP_{MAX}/PBP_{MOD} = \sum(MSH_{REC} + MSH_{RES}), \quad (5)$$

$$PBP_{MIN} = \sum(MSH_{REC} + MSH_{RES}), \quad (6)$$

where MSH_{REC}, MSH_{RES}, H_{REC}, and H_{RES} represent the proportion of maximum sustainable harvest (MSH) in the recoverable pool, the proportion of MSH in the residual pool, the proportion of current harvest (H) in the recoverable pool, and the proportion of H in the residual pool, respectively. PBP_{CAP} was calculated as the sum of all vegetated pixels, PBP_{MAX} excluded unavailable sources, PBP_{MOD} excluded unavailable and low-availability sources, and PBP_{MIN} was calculated as the sum of only immediately available sources, respectively (table 1). A summary of the calculated global agricultural and forest bioenergy potential pools are presented as a function of region in supplemental tables S4 and S5, respectively, available online at *http://dx.doi.org/10.1525/bio.2012.62.8.11*.

Table 2. Global area, net primary productivity, and primary bioenergy potential as a function of landcover type.

			NPP			Yield	
Landcover type	**Area[a]**	**NPP[b]**	**Mean[c]**	**SD**	**PBP[d]**	**Mean[e]**	**SD**
Crop	15.2	6.6	434	229	143.9	9.5	5.0
Pasture	17.8	8.5	478	298	184.3	10.4	6.3
Accessible range	9.6	5.6	583	280	121.8	12.7	6.1
Remote range	12.9	4.3	333	197	92.3	7.1	4.2
Protected range	1.6	0.7	438	259	14.8	9.3	5.5
Accessible forest	14.7	12.4	844	412	67.3	4.5	2.2
Remote forest	14.9	10.7	718	398	55.9	3.8	2.1
Protected forest	3.1	2.8	903	404	14.4	4.7	2.1
Low productivity	20.3	1.5	74	42	32.8	1.6	0.9
Total or average	110.1	53.1	482	402	727.5	6.6	5.5

Abbreviations: NPP, net primary production; PBP, primary bioenergy potential; SD, standard deviation.
[a]In millions of square kilometers. [b]In petagrams of carbon per year. [c]In grams of carbon per square meter per year. [d]In exajoules per year. [e]In megajoules per square meter per year.

in the range of previously reported values: 59 and 46 Pg C per year, reported by Haberl and colleagues (2007) and Del Grosso and colleagues (2008), respectively. Croplands were estimated to account for 6.6 Pg C per year over 15.2 million km^2 (table 2, figure 1), which is comparable to the estimates of 6.8 Pg C per year over 14.5 million km^2 and 6.3 Pg C per year over 15.2 million km^2 reported by Haberl and colleagues (2010) and Field and colleagues (2008), respectively. The current total cropland harvest (H_{TOTAL}) was estimated as 5.5 Pg C per year over 15.2 million km^2 (table S2, figure S2), which is again within the range of values reported by Haberl and colleagues (2007). *Harvested forestland*, defined as accessible forestland, had an associated NPP of 12.4 Pg C per year over 14.7 million km^2 (table 2, figure 1). Although forestry area varies significantly by definition, we report a total forest harvest (H_{TOTAL}) of 0.95 Pg C per year (table S3, figure S2), which is consistent with the estimates of 1.0 and 1.1 Pg C per year reported by Haberl and colleagues (2010) and Vitousek and colleagues (1986), respectively.

Global primary bioenergy potential

We estimated the biospheric capacity for bioenergy (PBP_{CAP}) to be 727.5 exajoules (EJ) per year over 110.1 million km^2 (table 3a, figure 3). With the removal of unavailable sources (i.e., current crop and forestry harvest, protected land, and low-productivity areas), PBP_{MAX} was reduced to 548.4 EJ per year over 55.2 million km^2, with an associated yield-potential range from 3.0 to 14.8 MJ per m^2 per year (table 3a, figure 3). Regionally, sub-Saharan Africa (26.8%), South America (24.2%), North America (11.1%), Eastern Europe (9.5%), and Central Asia (6.5%) accounted for 78.1% of the total PBP_{MAX} (figure 4). The removal of low-availability sources (i.e., accessible forest, pastures, and remote regions) resulted in a PBP_{MOD} of 180.4 EJ per year over 9.6 million km^2 (table 3a, figure 3). However, the yield-potential range increased to 6.6–18.8 MJ per m^2 per year (table 3a, figure 3). Regional contributions also changed, with sub-Saharan Africa (28.9%), South America (15.4%), North America (11.9%), Western Europe (11.4%), and Central Asia (7.2%) accounting for 74.8% of the total PBP_{MOD} (figure 4). Finally, considering only immediately available sources (i.e., current crop and forestry residuals), PBP_{MIN} was reduced to 58.6 EJ per year (table 3a, figure 3). PBP_{MIN} is highly dependent on the proportion of harvested losses considered *recoverable*, which is still relatively unresolved in the literature (Haberl et al. 2010). Nonetheless, our estimate of PBP_{MIN} is within the range reported in the current literature and is therefore representative of current estimates (table 3b; Haberl et al. 2010). Western Europe (17.9%), North America (16.8%), South Asia (11.8%), sub-Saharan Africa (10.3%), and Central Asia (9.9%) were estimated to account for 66.7% of the total PBP_{MIN} (figure 4).

Global primary bioenergy and yield potential

We calculated the maximum PBP to range from 35% to 108% of GPEC09 (figure 3; USEIA 2011). A main driver of PBP was average yield potential, which varied with land-use scenario from 6.6 to 12.7 MJ per m^2 per year, a range roughly four times lower than multiple previously published estimates (table 3b). For instance, Smeets and colleagues (2007) used an average yield-potential range of 29–39 MJ per m^2 per year to conclude that maximum global bioenergy potential could reach nearly 300% of GPEC09 by the year 2050 (table 3b, figure 5). Smeets and colleagues (2007) assumed steadily increasing yields, as well as the availability of the most advanced management practices (e.g., irrigation and fertilization). Similarly, Beringer and colleagues (2011) estimated irrigated yield potentials for the year 2050 to range from 33 to 40 MJ per m^2 per year, although significantly less land was considered *available* for bioenergy production (table 3b, figure 5). Finally, Pacca and Moreira (2011) used an average yield-potential value of 69 MJ per m^2 per year—the present-day yield potential for sugarcane grown under optimum nutrient availability, temperature, and water availability—to suggest that all the world's automobiles could be powered using only 4% of global croplands (table 3b, figure 5). These studies include different methodological assumptions and involve different time frames (table 3b, figure 5); however, they used yield potentials near the upper end of literature-derived estimates, mainly because of the shared assumption of the availability of management practices to mitigate biophysical constraints on crop productivity and yield.

We have shown that these studies used average yields significantly greater than both current crop yields and natural yield potentials (table 3b, figure 5). Because global agricultural yields have been reported as generally less than natural productivity (Haberl et al. 2007), we argue that these analyses overestimate bioenergy potential by failing to realistically limit the potential for management to overcome natural biophysical constraints on yield potential (table 3b, figure 5). Management practices, especially irrigation, has

Table 3a. Primary bioenergy potential as a function of land-use scenario.

Land-use scenario	Area[a]	Yield range[b]	Primary energy[c]
Biospheric capacity (PBP_{CAP})[d]	110.1	1.1–12.1	727.5
Maximum land use (PBP_{MAX})[d]	55.2	3.0–14.8	489.8
Moderate land use (PBP_{MOD})[d]	9.6	6.6–18.8	121.8
Minimum land use (PBP_{MIN})	—	—	58.6

[a]In millions of square kilometers.
[b]The yield range (in megajoules per square meter per year) represents a range of one standard deviation.
[c]In exajoules per year.
[d]PBP_{CAP}, PBP_{MAX}, and PBP_{MOD} are reported without the inclusion of harvest residual (PBP_{MIN}).

Table 3b. Current and future (approximately 2050) primary bioenergy potential estimates from the literature.

Reference	Source	Area (in millions of kilometers)	Yield range (in megajoules per square meter per year)	Primary energy (in exajoules per year)
Current				
Pacca et al. 2011	Sugarcane crop	0.7	69	46
Field et al. 2008	Abandoned crop	3.9	6.9	27
Campbell et al. 2008	Abandoned crop	3.9–4.7	8–9	32–41
Approximately 2050				
Haberl et al. 2012	Maximum crop	3.8–9.9	11–14	40–133
Haberl et al. 2012	Residuals crop	—	—	24–28
Beringer et al. 2011, irrigated	Maximum crop	1.4–4.5	33–40	52–174
Beringer et al. 2011, rainfed	Maximum crop	1.4–4.5	18–26	26–116
Erb et al. 2009	Maximum crop	2.3–9.9	12–13	28–128
Van Vuuren et al. 2009	Maximum crop	0.0–6.0	20–60	65–300
Smeets et al. 2007	Maximum crop	7.3–35.9	29–39	215–1272
Hoogwijk et al. 2005	Maximum crop	29–37	10–18	300–650
Literature reviews				
Chum et al. 2011	All available	—	—	120–300
Dornburg et al. 2010	All available	—	—	120–330
Haberl et al. 2010	All available	—	—	160–270
Haberl et al. 2010	All residues	—	—	15–84

[a]Yield range represents a range of one standard deviation.

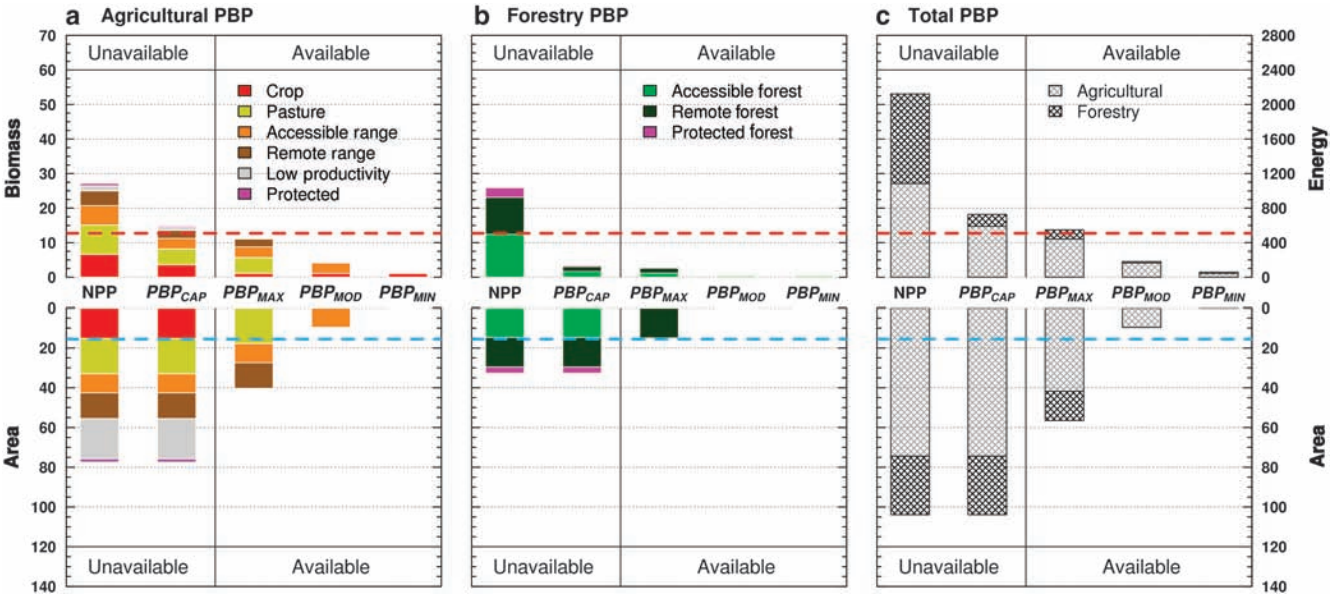

Figure 3. Primary bioenergy potential (PBP) and the corresponding land area requirements as a function of land-use scenario. **PBP_{CAP}, PBP_{MAX}, PBP_{MOD}, PBP_{MIN}** ***represent land-use scenarios defined according to table 1. The land-use scenarios are divided into*** **available** ***and*** **unavailable** ***groups on the basis of whether unavailable sources (i.e., current crop and forest harvest, protected regions, and land under a minimum productivity threshold) were considered (table 1). For a comparison, 2009 global primary energy consumption (509 exajoules) and current cropland area (15.2 millions of square kilometers) are represented by red and blue dashed lines, respectively. (a) PBP on agricultural lands, defined to include crop, pasture, accessible range, remote range, and protected range. (b) PBP on forestry land, defined to include accessible forests, remote forests, and protected forests. (c) PBP on all land, divided between agricultural and forestry land. Biomass is expressed in petagrams of carbon per year, area is in millions of square kilometers, and energy is in exajoules per year. Abbreviations and variables: NPP, net primary productivity;*** **PBP_{CAP},** ***biospheric capacity for bioenergy;*** **PBP_{MAX},** ***PBP for the maximum land-use scenario;*** **PBP_{MIN},** ***PBP for the minimum land-use scenario;*** **PBP_{MOD},** ***PBP for the moderate land-use scenario.***

been observed to increase productivity above natural rates over relatively localized areas (DeFries 2002, Haberl et al. 2007). Therefore, increases in yield potential above the natural potential—as was reported by Beringer and colleagues (2011)—may be theoretically achievable (table 3b, figure 5). However, because of limited freshwater availability and the numerous detrimental effects of fertilization, maintaining yield potentials at levels higher than natural rates of productivity would probably be unsustainable over large spatial scales (see the "Natural productivity as a yield-potential constraint" section).

In contrast, our yield-potential estimates are consistent with those from studies in which more restrictive assumptions were used regarding management practices and the influence of biophysical factors on yield potential (table 3b, figure 5; Hoogwijk et al. 2005, Campbell et al. 2008, Field et al. 2008, Erb et al. 2009, Haberl et al. 2012). Campbell and colleagues (2008) and Field and colleagues (2008) used satellite-derived NPP to calculate current yield potential on degraded agricultural land and reported yield-potential values at the lower end of the yield range reported here (table 3b, figure 5). We attribute this difference to differing landcover assumptions, because degraded lands are known to experience relatively low productivity. Hoogwijk and colleagues (2005) estimated crop-specific yield potentials for the year 2050 using a process model driven by climate data and documented yield-potential values at the high end of our reported range (table 3b, figure 5). However, even these yield-potential estimates may still be unrealistic, because our estimates represent upper-envelope natural yield potentials and are likely to overestimate the potential for crop-specific yields (Haberl et al. 2007). This is most apparent in figure 5, in which the trends in productivity on agricultural lands are shown to be significantly less than the productivity trends for all PBP scenarios.

Global primary bioenergy and land use

We estimated maximum land availability for bioenergy cultivation to range from 9% to 50% of total vegetated land area (figure 3), which is at the upper end of the range of values in recent studies (table 3b, figure 5). Because our goal was an upper-envelope evaluation of bioenergy potential, we included landcover classes often removed by previous studies, such as remote regions and pastures. Bioenergy cultivation on these low-availability landcover types has many associated trade-offs. Expansion into remote regions represents

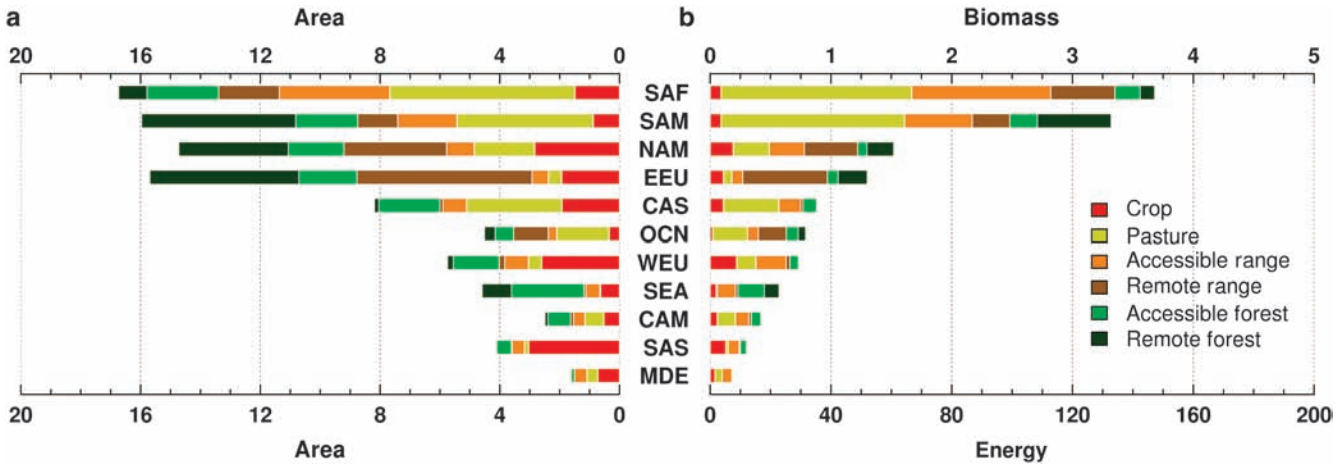

Figure 4. Primary bioenergy potential (PBP) and the corresponding land area requirements as a function of region. The regions were aggregated according to the classification of the geographical macroregions and geographic subregions as defined by the United Nations Statistical Division (see supplemental figure S1, available online at* http://dx.doi.org/10.1525/bio.2012.62.8.11*). (a) Maximum land use (*PBP_{MAX}*), defined to include all vegetated land, excluding unavailable sources (table 1). (b) Maximum primary bioenergy potential (*PBP_{MAX}*), estimated using net primary productivity data from NASA's Moderate-Resolution Imaging Spectroradiometer as an upper-envelope constraint. Area is expressed in millions of kilometers, biomass is in petagrams of carbon per year, and energy is in exajoules per year. Abbreviations: CAM, Central America; CAS, Central Asia; EEU, Eastern Europe; MDE, Middle East; NAM, North America; OCN, Oceania and Australia; SAF, sub-Saharan Africa; SAM, South America; SAS, South Asia; SEA, Southeast Asia; WEU, Western Europe (figure S1).

roughly 20% of global bioenergy potential (table 2, figure 3); however, infrastructure establishment and land conversion in these regions would require large-scale fossil fuel energy inputs, which would result in a significant initial carbon debt in setting up these bioenergy systems (Fargione et al. 2008). Remote regions are distributed over 27.8 million km^2 (table 2), which means that to reach the full energy potential of these regions, a network of access roads would be required over an area greater than the total extent of North America. In addition, because the average yield potential on remote land is relatively low (table 2, figure 3), the associated time required to offset the initial fossil fuel inputs would be significant, which decreases the attractiveness of remote regions (Fargione et al. 2008).

More notable, pastures were estimated to account for nearly half of global bioenergy potential over an area of 17.8 million km^2—an area larger than the total extent of South America (table 2, figure 3). Potential may exist for the conversion of pastures to bioenergy-production land, because only roughly 20% of annual aboveground productivity is consumed by grazers (Haberl et al. 2007). However, conversion of pasturelands has already been associated with significant detrimental impacts (McAlpine et al. 2009, Arima et al. 2011). For instance, Arima and colleagues (2011) documented that deforestation rates in the Brazilian Amazon were indirectly associated with pastureland displacement by bioenergy plantations (i.e., indirect land-use change). Given that global meat consumption continues to rise (McAlpine et al. 2009), the detrimental impacts associated with pastureland-to-bioenergy conversion are likely to only increase in the future (McAlpine et al. 2009, Arima et al. 2011).

In contrast, in considering only current harvest residues, we estimated a bioenergy potential (PBP_{MIN}) equivalent to 12% of GPEC09 (table 3a, figure 3). Residuals are an attractive potential energy source because they are currently accessible and do not require additional land use, which reduces the significance of their detrimental impacts (e.g., carbon debt and indirect land-use change). Because current global bioenergy use accounts for approximately 10% of GPEC09 (Haberl et al. 2010), the use of current harvest residuals has the potential to more than double current global bioenergy use. Potentially easily developed sources of residual bioenergy include forestry slash piles, agricultural field residues, and forestry postprocessing sawdust and debris (Haberl et al. 2010). However, to fully reach the above-mentioned 12% GPEC09 offset, we estimate that residuals would have to be harvested over 29.9 million km^2—an area greater than the total extent of North America (table 3b).

Natural productivity as a yield-potential constraint

We based our analysis on the assumption that natural rates of productivity represent an upper-envelope constraint on bioenergy potential, which raises the question of what the potential is for increasing productivity above natural rates. Enhancing productivity beyond the natural potential would require either increased efficiency of light capture

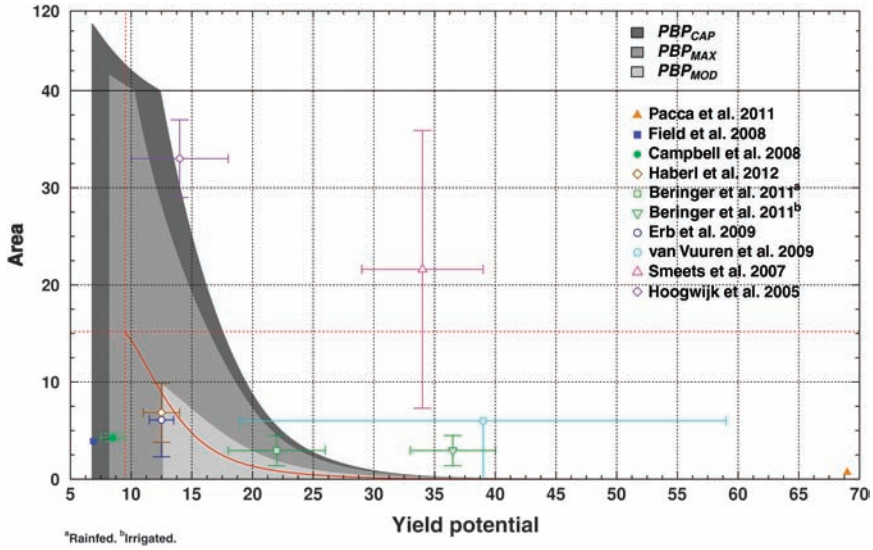

Figure 5. Cumulative maximum yield potential (in megajoules [MJ] per square meter per year) as a function of area (in millions of square kilometers) and land-use scenario. **PBP_{CAP}, PBP_{MAX},** ***and*** **PBP_{MOD}** ***represent the cumulative maximum yield-potential curves for each land-use scenario, which are described in table 1. We calculated cumulative maximum yield potential by sorting all 10-square-kilometer (km^2)–resolution yield-potential pixel values for a given scenario from highest to lowest and then averaging over the highest yield values for a given land area. Therefore, for any given land area from 10 km^2 to 110 million km^2, the corresponding value of the curve represents the maximum yield potential for that given area. As a comparison, the current cropland cumulative maximum yield potential is represented by the red solid line. Total cropland area (15.2 million km^2) and the corresponding maximum yield (9.5 MJ per square meter per year) are represented by red dotted lines. In addition, the area and corresponding yield-potential estimates from recent bioenergy analyses are displayed as mean values with whiskers denoting the full range of values considered in the study. Studies that were focused on current conditions are represented by solid symbols, whereas those based on the year 2050 are represented by open symbols (see table 3b for more detail). We show that a number of recent studies used yield-potential values higher than maximum natural yield potentials, which we attribute to overoptimistic assumptions regarding the availability of management practices or to an unrealistic consideration of biophysical constraints on yield potential.***

(light-interception efficiency) or enhanced efficiency of the conversion of captured light into biomass (light-use efficiency), neither of which are likely near-future scenarios. Under optimal growing conditions (i.e., no temperature, moisture, or nutrient constraints), Long and colleagues (2006) suggested light-interception efficiency as near a theoretical maximum for major crops, leaving only light-use efficiency as a mechanism to increase productivity. However, despite a long history, genetic manipulation by plant breeding has yet to significantly enhance light-use efficiency per unit area (Richards 2000), which partially explains why agricultural yield-increase rates have been declining since the Green Revolution (Funk and Brown 2009). Next-generation bioenergy crops such as perennial rhizomatous grasses (PRGs; e.g., *Panicum*, *Miscanthus*) are fundamentally different from food crops in that they use the C_4 photosynthesis pathway, which significantly improves light-use efficiency and maximizes productivity (Heaton et al. 2004). However, PRGs achieve higher light-use efficiency at the cost of energy (Heaton et al. 2004), which reduces their competitive advantage in suboptimal growing conditions (e.g., in nutrient-poor, dry, or cold climates). Therefore, PRGs could significantly increase yields in agricultural systems in which less-efficient food crops are currently grown and in which nearly optimal conditions are maintained (Heaton et al. 2008). On natural landscapes however, C_4 species are already distributed according to climate and nutrient availability, which limits the potential of PRGs to improve natural productivity without fertilization or irrigation inputs.

Under suboptimal growing conditions, light-use efficiency can be increased by reducing growth constraints (e.g., temperature, precipitation, nutrients) through management (e.g., irrigation, fertilization), which results in increased photosynthesis per unit of time (Long et al. 2006). However, evidence suggests that the global rates of irrigation and fertilization are approaching peak levels in many regions, with significant associated detrimental impacts. For instance, global groundwater depletion more than doubled from 1960 to 2000, mainly because of increased rates of irrigation (Wada et al. 2010). Given that 40% of the global food supply comes from irrigation-dependent croplands (Gleick 2003), a more likely scenario for the future may be *decreased* global yield potentials as irrigation limits are reached and droughts become more frequent (Gleick 2003, Wada et al. 2010, Dai 2011). Similarly, current fertilization demand has more than doubled global reactive nitrogen availability, which has resulted in extensive eutrophication of freshwater and coastal zones, along with increased emission of the potent greenhouse gas nitrous oxide, a trace gas with a global warming potential roughly 300 times greater than an equal mass of carbon dioxide (Galloway et al. 2008). Therefore, any productivity increases associated with future increases in irrigation or fertilization will be at the cost of freshwater

pollution and, possibly, greenhouse gas emissions (Galloway et al. 2008, Wada et al. 2010).

Conclusions

We calculate maximum global bioenergy potential to range from 35% to 108% of GPEC09 (figure 3). However, a number of key assumptions and factors need to be considered in order to determine the difference between *maximum* and a *realistic maximum* bioenergy potential. Our upper-end maximum calculation (PBP_{MAX}) required the conversion of 55.6 million km^2 of natural vegetation for bioenergy production, an area more than the total extent of Asia and Europe combined, whereas our lower-end maximum calculation (PBP_{MOD}) required the conversion of 9.6 million km^2 of natural vegetation, an area nearly equivalent to the total extent of Europe. Even the complete use of current harvest residues (PBP_{MIN}) was shown to require biomass collection over 29.9 million km^2, an area greater than the total extent of North America. Given the scale associated with these scenarios, we conclude that the realistic maximum global bioenergy potential ranges somewhere between 12% of GPEC09—the potential associated with current harvest residuals (PBP_{MIN})—and 35% of GPEC09—the lower-end maximum calculation (PBP_{MOD}). By 2050, global primary energy demand is projected to more than double (Haberl et al. 2010); we therefore estimate that the realistic maximum contribution of bioenergy ranges roughly from 5% to 15% of our future energy needs. We do not advocate global bioenergy production at the levels reported in this analysis; instead, we have simply reported an upper-envelope constraint for PBP on the basis of existing satellite observations of global vegetation productivity.

Acknowledgments

We thank Norman L. Miller for his support in funding this research and Cory C. Cleveland for providing valuable suggestions. This work was supported by Energy Biosciences Institute grant no. 007J49 and NASA Earth Observing System Moderate-Resolution Imaging Spectroradiometer project grant no. NNH09ZDA001N-TERRA-AQUA.

References cited

Arima EY, Richards P, Walker R, Caldas MM. 2011. Statistical confirmation of indirect land use change in the Brazilian Amazon. Environmental Research Letters 6 (2, art. 024010). doi:10.1088/1748-9326/6/2/024010

Beringer T, Lucht W, Schaphoff S. 2011. Bioenergy production potential of global biomass plantations under environmental and agricultural constraints. Global Change Biology Bioenergy 3: 299–312.

Campbell JE, Lobell D, Genova R, Field CB. 2008. The global potential of bioenergy on abandoned agricultural lands. Environmental Science and Technology 42: 5791–5795.

Chum H, et al. 2011. Bioenergy. Pages 23–41 in Edenhofer O, et al., eds. IPCC Special Report on Renewable Energy Sources and Climate Change Mitigation (SRREN). Intergovernmental Panel on Climate Change.

Dai A. 2011. Drought under global warming: A review. Wiley Interdisciplinary Reviews: Climate Change 2: 45–65.

DeFries R. 2002. Past and future sensitivity of primary production to human modification of the landscape. Geophysical Research Letters 29. doi:10.1029/2001GL013620

Del Grosso S, Parton W, Stohlgren T, Zheng D, Bachelet D, Prince S, Hibbard K, Olson R. 2008. Global potential net primary production predicted from vegetation class, precipitation, and temperature. Ecology 89: 2117–2126.

Erb K-H, Haberl H, Krausmann F, Lauk C, Plutzar C, Steinberger JK, Müller C, Bondeau A, Waha K, Pollack G. 2009. Eating the planet: Feeding and fueling the world sustainably, fairly, and humanely—A scoping study. Institute of Social Ecology, Potsdam Institute of Climate Impact Research.

Fargione J, Hill J, Tilman D, Polasky S, Hawthorne P. 2008. Land clearing and the biofuel carbon debt. Science 29: 1235–1238.

Field CB, Campbell JE, Lobell D. 2008. Biomass energy: The scale of the potential resource. Trends in Ecology and Evolution 23: 65–72.

Friedl MA, Sulla-Menashe D, Tan B, Schneider A, Ramankutty N, Sibley A, Huang X. 2010. MODIS Collection 5 global land cover: Algorithm refinements and characterization of new datasets. Remote Sensing of Environment 114: 168–182.

Funk CC, Brown ME. 2009. Declining global per capita agricultural production and warming oceans threaten food security. Food Security 1: 271–289.

Galloway JN, Townsend AR, Erisman JW, Bekunda M, Cali Z, Freney JR, Martinelli LA, Seitzinger SP, Sutton MA. 2008. Transformation of the nitrogen cycle: Recent trends, questions, and potential solutions. Science 320: 889–892.

Gleick PH. 2003. Water use. Annual Review of Environmental Resources 28: 275–314.

Gregg JS, Smith SJ. 2010. Global and regional potential for bioenergy from agricultural and forestry residue biomass. Mitigation and Adaptation Strategies for Global Change 15: 241–262.

Haberl H, Erb K-H, Krausmann F, Gaube V, Bondeau A, Plutzar C, Gingrich S, Lucht W, Fisher-Kowalski M. 2007. Quantifying and mapping the human appropriation of net primary production in Earth's terrestrial ecosystems. Proceedings of the National Academy of Sciences 104: 12942–12947.

Haberl H, Beringer T, Bhattacharya SC, Erb K-H, Hoogwijk M. 2010. The global technical potential of bio-energy in 2050 considering sustainability constraints. Current Opinion in Environmental Sustainability 2: 394–403.

Haberl H, Erb K-H, Krausmann F, Bodeau A, Lauk C, Müller C, Plutzar C, Steinberger JK. 2011. Global bioenergy potentials from agricultural land in 2050: Sensitivity to climate change, diets and yields. Biomass and Bioenergy 35: 4753–4769.

Heaton E[A], Voigt T, Long SP. 2004. A quantitative review comparing the yields of two candidate C_4 perennial biomass crops in relation to nitrogen, temperature, and water. Biomass and Bioenergy 27: 21–30.

Heaton EA, Dohleman FG, Long SP. 2008. Meeting US biofuel goals with less land: The potential of *Miscanthus*. Global Change Biology 14: 2000–2014.

Hoogwijk M, Faaij A[PC], Eickhout B, de Vries B, Turkenburg W[C]. 2005. Potential of biomass energy out to 2100, for four IPCC SRES land-use scenarios. Biomass and Bioenergy 29: 225–257.

Johnston M, Foley JA, Holloway T, Kucharik C, Monfreda C. 2009. Resetting global expectations from agricultural biofuels. Environmental Research Letters 4 (1, art. 014004). doi:10.1088/1748-9326/4/1/014004

Long SP, Zhu XG, Naidu SL, Ort DR. 2006. Can improvement in photosynthesis increase crop yields? Plant Cell and Environment 29: 315–330.

McAlpine CA, Etter A, Fearnside PM, Seabrook L, Laurance WF. 2009. Increasing world consumption of beef as a driver of regional and global change: A call for policy action based on evidence from Queensland (Australia), Colombia, and Brazil. Global Environmental Change 19: 21–33.

Monfreda C, Ramankutty N, Foley JA. 2008. Farming the planet: 2. Geographic distribution of crop areas, yields, physiological types,

and net primary production in the year 2000. Global Biogeochemical Cycles 22 (art. GB1022). doi:10.1029/2007GB002947

Nonhebel S. 2002. Energy yields in intensive and extensive biomass production systems. Biomass and Bioenergy 22: 159–167.

Pacca S, Moreira JR. 2011. A biorefinery for mobility? Environmental Science and Technology 45: 9498–9505.

Ramankutty N, Evan AT, Monfreda C, Foley JA. 2008. Farming the planet: 1. Geographic distribution of global agricultural lands in the year 2000. Global Biogeochemical Cycles 22 (art. GB1003). doi:10.1029/2007GB002952

Richards RA. 2000. Selectable traits to increase crop photosynthesis and yield of grain crops. Journal of Experimental Botany 51 (suppl. 1): 447–458.

Roy J, Saugier B, Mooney HA, eds. 2001. Terrestrial Global Productivity. Academic.

Running SW, Nemani RR, Heinsch FA, Zhao M, Reeves M, Hashimoto H. 2004. A continuous satellite-derived measure of global terrestrial primary production. BioScience 54: 547–560.

Schmer MR, Vogel KP, Mitchell RB, Perrin RK. 2008. Net energy of cellulosic ethanol from switchgrass. Proceedings of the National Academy of Sciences 105: 464–469.

Schubert SD, Rood RB, Pfaendtner J. 1993. An assimilated dataset for Earth science applications. Bulletin of the American Meteorological Society 74: 2331–2342.

[SEDAC] Socioeconomic Data and Applications Center. 2005. Last of the wild data: Global human footprint data set, version 2. SEDAC. (17 July 2012; *http://sedac.ciesin.columbia.edu/wildareas/downloads.jsp*)

Smeets EMW, Faaij APC, Lewandowski IM, Turkenburg WC. 2007. A bottom-up assessment and review of global bio-energy potentials to 2050. Progress in Energy and Combustion Science 33: 56–106.

Smith WK, Cleveland CC, Reed SC, Miller NL, Running SW. 2012. Bioenergy potential of the United States constrained by satellite observations of existing productivity. Environmental Science and Technology 46: 3536–3544. doi:10.1021/es203935d

Tilman D, et al. 2009. Beneficial biofuels: The food, energy, and environment trilemma. Science 325: 270–271.

Tsubo M, Walker S, Mukhala E. 2001. Comparisons of radiation use efficiency of mono-/inter-cropping systems with different row orientations. Field Crops Research 71: 17–29.

[UNSD] United Nations Statistical Division. 2011. Composition of macro geographical (continental) regions, geographical sub-regions, and selected economic and other groupings. UNSD. (17 July 2012; *http://unstats.un.org*)

[USEIA] United States Energy Information Administration. 2011. International Energy Outlook 2011. United States Department of Energy. Report no. DOE/EIA-0484. (17 July 2012; *www.eia.gov/forecasts/ieo*)

Van Vuuren DP, van Vliet J, Stehfest E. 2009. Future bio-energy potential under various natural constraints. Energy Policy 37: 4220–4230.

Vitousek PM, Ehrlich PR, Ehrlich AH, Matson PA. 1986. Human appropriation of the products of photosynthesis. BioScience 36: 368–373.

Wada Y, van Beek LPH, van Kempen CM, Reckman, JWTM, Bierkens MFP. 2010. Global depletion of groundwater resources. Geophysical Research Letters 37 (art. L20402). doi:10.1029/2010GL044571

Williams K, Percival F, Merino J, Mooney HA. 1987. Estimation of tissue construction cost from heat of combustion and organic nitrogen content. Plant, Cell and Environment 10: 725–734.

Zhao M, Running SW. 2010. Drought-induced reduction in global terrestrial net primary production from 2000 through 2009. Science 329: 940–943.

———. 2011. Response to comments on "Drought-induced reduction in global terrestrial net primary production from 2000 through 2009." Science 333: 1093.

Zhao M, Heinsch FA, Nemani RR, Running SW. 2005. Improvements of the MODIS terrestrial gross and net primary production global data set. Remote Sensing of Environment 2: 164–176.

W. Kolby Smith (bill.smith@ntsg.umt.edu), Maosheng Zhao, and Steven W. Running are affiliated with the Numerical Terradynamic Simulation Group, in the Department of Ecosystem and Conservation Sciences, at the University of Montana, in Missoula.